

Constraint to chiral invariant masses of nucleons from GW170817 in an extended parity doublet model

Takahiro Yamazaki* and Masayasu Harada†

Department of Physics, Nagoya University, Nagoya 464-8602, Japan

(Received 18 January 2019; published 12 August 2019)

We construct nuclear matter based on an extended parity doublet model including four light nucleons, $N(939)$, $N(1440)$, $N(1535)$, and $N(1650)$. We exclude some values of the chiral invariant masses by requiring the saturation properties of normal nuclear matter: saturation density, binding energy, incompressibility, and symmetry energy. We find a further constraint on the chiral invariant masses from the tidal deformability determined by the observation of the gravitational waves from neutron star merger GW170817. Our result shows that the chiral invariant masses are larger than about 600 MeV. We also give some predictions on the symmetry energy and the slope parameters in the high density region, which will be measured in future experiments.

DOI: [10.1103/PhysRevC.100.025205](https://doi.org/10.1103/PhysRevC.100.025205)

I. INTRODUCTION

Chiral symmetry and its spontaneous breaking is one of the important features in low-energy hadron physics based on QCD. The breaking generates a part of hadron mass and causes a splitting between chiral partners. It is interesting to ask how much of the nucleon mass is generated by spontaneous chiral symmetry breaking and what is the chiral partner to the nucleon.

In Ref. [1], a model based on the parity doublet structure was introduced, where the excited nucleon $N(1535)$ is regarded as the chiral partner to the nucleon $N(939)$. It is important to note that their masses include a chiral invariant mass in addition to the mass caused by spontaneous chiral symmetry breaking. The determination of the chiral invariant mass using the phenomenology at vacuum is done in, e.g., Refs. [2–4], and shows that the chiral invariant mass of the nucleon is smaller than about 500 MeV.

The parity doublet structure is extended to include hyperons and/or more nucleons in, e.g., Refs. [5–17]. In Ref. [17], the authors of the present paper constructed a model which includes two chiral representations, the $[(\mathbf{2}, \mathbf{3}) \oplus (\mathbf{3}, \mathbf{2})]$ representation under $SU(2)_L \otimes SU(2)_R$ in addition to the $[(\mathbf{1}, \mathbf{2}) \oplus (\mathbf{2}, \mathbf{1})]$ representation, to study four nucleons, $N(939)$, $N(1440)$, $N(1535)$, and $N(1650)$. It was shown that there are wide range of two chiral invariant masses satisfying vacuum properties of the nucleons—the masses, the axial charges and the pionic decay widths—and that the solutions are categorized into five groups.

The properties of hot and/or dense matter, including neutron star matter based on the parity doublet structure, are widely studied in Refs. [11,18–36]. In [11,18–22,24,26,28], the authors studied the relation between the chiral invariant

mass and the incompressibility K of nuclear matter, and their results show that the empirical value $K \approx 240$ MeV only when the chiral invariant mass is close to nucleon's mass, $m_0 \approx 900$ MeV. In Ref. [29], six-point interaction of scalar mesons was introduced and it was shown that the saturation properties are reproduced for a wide region of the chiral invariant mass, i.e., $500 \leq m_0 \leq 900$ MeV. In Ref. [36], the constraint on the chiral invariant mass from the properties of neutron stars, including the tidal deformability observed from GW170817 [37–39], was obtained as 780–810 MeV. Recently, the parity doublet model was used to study nuclei with finite size in Ref. [40], which showed that $m_0 \sim 700$ MeV is preferred to reproduce the properties of nuclei. The relatively large value of the chiral invariant mass seems also consistent with lattice analyses in Refs. [41–43].

In this paper, we construct nuclear matter and neutron star matter using the model introduced in Ref. [17] based on the mean field approximation. For the meson parts, we use the model introduced in Ref. [29]; the six-point interaction of the scalar field is introduced and the ω and ρ mesons are included based on the hidden local symmetry [44,45]. We will show that requiring the saturation properties of normal nuclear matter excludes some combinations of two chiral invariant masses. We solve the Tolman-Oppenheimer-Volkov (TOV) equation [46,47] to determine the energy density and tidal deformability of neutron stars. Then, we will show that the tidal deformability observed from GW170817 [37–39] provides a further constraint on the chiral invariant masses.

This paper is organized as follows: In Sec. II, we include the ω and ρ mesons in the model introduced in Ref. [17]. We give formulations to study nuclear matter in the mean field approximation in Sec. III. Here we show formulas to study saturation properties of normal nuclear matter and the equation of state for neutron star matter. Section IV is devoted to the main part where we obtain constraints on the chiral invariant masses from the saturation properties and tidal deformability from GW170817. We also provide predictions

*yamazaki@hken.phys.nagoya-u.ac.jp

†harada.masayasu@nagoya-u.jp

for the relations between the mass and radius as well as for the mass and the central density of neutron stars and for the symmetry energy and the slope parameter in dense matter. Finally, we give a summary and discussions in Sec. V.

II. MODEL

In this section, we introduce an extended parity doublet model to describe nuclear matter based on the model constructed in Ref. [17]. The model includes four baryon fields corresponding to the following representations under $SU(2)_L \times SU(2)_R$ chiral symmetry:

$$\begin{aligned} \psi_{1l} &\sim (\mathbf{2}, \mathbf{1}), & \psi_{1r} &\sim (\mathbf{1}, \mathbf{2}), \\ \psi_{2l} &\sim (\mathbf{1}, \mathbf{2}), & \psi_{2r} &\sim (\mathbf{2}, \mathbf{1}), \\ \eta_{1l} &\sim (\mathbf{2}, \mathbf{3}), & \eta_{1r} &\sim (\mathbf{3}, \mathbf{2}), \\ \eta_{2l} &\sim (\mathbf{3}, \mathbf{2}), & \eta_{2r} &\sim (\mathbf{2}, \mathbf{3}). \end{aligned} \quad (1)$$

The isosinglet scalar meson σ and the isotriplet pseudoscalar meson π are included in a matrix field M , which transforms as

$$M \rightarrow g_L M g_R^\dagger, \quad (2)$$

where $g_{L,R} \in SU(2)_{L,R}$. Following Ref. [29], we include ω and ρ mesons as the gauge bosons of hidden local symmetry [44,45] by performing the polar decomposition of the field M as¹

$$M = \xi_L^\dagger \frac{\sigma}{2} \xi_R = \frac{\sigma}{2} \xi_L^\dagger \xi_R = \frac{\sigma}{2} U. \quad (3)$$

We introduce the same potential for M as used in Ref. [29]:

$$\begin{aligned} V_M &= -\bar{\mu}^2 \text{tr}[MM^\dagger] + \lambda_4 [\text{tr}[MM^\dagger]]^2 - \frac{4}{3} \lambda_6 [\text{tr}[MM^\dagger]]^3 \\ &\quad - \frac{1}{2} \epsilon (\text{tr}[\mathcal{M}^\dagger M] + \text{tr}[\mathcal{M} M^\dagger]), \end{aligned} \quad (4)$$

where ϵ is a parameter with dimension 2 and \mathcal{M} is the quark mass matrix defined as

$$\mathcal{M} = \begin{pmatrix} m_u & 0 \\ 0 & m_d \end{pmatrix} \quad (5)$$

with m_u and m_d being the masses of up and down quarks. In the present analysis, we neglect the difference between these masses, and take $m_u = m_d = \bar{m}$. In vacuum, the combination $\bar{m}\epsilon$ is related to the pion mass as

$$\bar{m}\epsilon = m_\pi^2 f_\pi. \quad (6)$$

We adopt the Yukawa interaction terms among M and the nucleons as in Ref. [17], so that we omit those in this paper.

We introduce the interaction terms among the vector mesons and nucleons similarly to Ref. [29]. Here, instead of writing the full Lagrangian, we shall show the relevant terms in the present analysis. The resultant interaction term for the ω meson is written as

$$\mathcal{L}_{\omega N} = -g_\omega \left(\sum_{i=1,2} \bar{\psi}_i \boldsymbol{\tau} \cdot \boldsymbol{\rho} \psi_i + \sum_{j=1,2} \bar{\eta}_j \boldsymbol{\tau} \cdot \boldsymbol{\rho} \eta_j \right). \quad (7)$$

Here we assume that the coupling to ψ is the same as that to η for simplicity. Similarly, the interaction for ρ mesons is given by

$$\mathcal{L}_{\rho N} = -\frac{1}{2} g_\rho \left(\sum_{i=1,2} \bar{\psi}_i \boldsymbol{\tau} \cdot \boldsymbol{\rho} \psi_i + \sum_{j=1,2} \bar{\eta}_j \boldsymbol{\tau} \cdot \boldsymbol{\rho} \eta_j \right). \quad (8)$$

We note that the mass terms for ω and ρ mesons are written as

$$V_\omega = -\frac{1}{2} m_\omega^2 \omega_\mu \omega^\mu, \quad V_\rho = -\frac{1}{2} m_\rho^2 \rho_\mu \rho^\mu. \quad (9)$$

III. FORMULATION

In this section, we present formulations to study nuclear matter in the mean field approximation based on the model introduced in the previous section. Here we assume that all the parameters of the model do not depend on the chemical potentials.

A. Thermodynamic potential

In the present analysis, we assume that there are no neutral and charged pion condensations, and that the fields have their vacuum expectation values (VEVs) as

$$\sigma = \sigma_0, \quad \omega_{\mu=0} = \omega, \quad \rho_{\mu=0}^3 = \rho. \quad (10)$$

In the mean field approximation, the thermodynamic potential is obtained by

$$\Omega = \sum_{i=1,2,3,4, N=p,n} \Omega_{N^{(i)}} + V_M + V_\omega + V_\rho, \quad (11)$$

where

$$V_M = -\frac{\bar{\mu}^2}{2} \sigma_0^2 + \frac{\lambda_4}{4} \sigma_0^4 - \frac{\lambda_6}{6} \sigma_0^6 - m_\pi^2 f_\pi \sigma_0, \quad (12)$$

$$V_\omega = -\frac{1}{2} m_\omega^2 \omega^2, \quad (13)$$

$$V_\rho = -\frac{1}{2} m_\rho^2 \rho^2. \quad (14)$$

The contribution from the nucleons, $\Omega_{N^{(i)}}$ is expressed as

$$\Omega_{N^{(i)}} = 2 \int \frac{d^3k}{(2\pi)^3} (E_N^{(i)} - \bar{\mu}_N^{(i)}) \theta(\bar{\mu}_N^{(i)} - E_N^{(i)}), \quad (15)$$

where $\theta(x)$ is the step function defined as

$$\theta(x) = \begin{cases} 1 & (x > 0), \\ 0 & (x < 0), \end{cases} \quad (16)$$

$E_N^{(i)}$ is an energy of the nucleon

$$E_N^{(i)} = \sqrt{k^2 + (m_N^{(i)})^2}. \quad (17)$$

$\bar{\mu}_N^{(i)}$ is the effective chemical potential defined by

$$\bar{\mu}_p^{(i)} = \bar{\mu}_B + \frac{1}{2} \bar{\mu}_I, \quad \bar{\mu}_n^{(i)} = \bar{\mu}_B - \frac{1}{2} \bar{\mu}_I, \quad (18)$$

with

$$\bar{\mu}_B = \mu_B - g_\omega \omega, \quad \bar{\mu}_I = \mu_I - g_\rho \rho. \quad (19)$$

¹The normalization of the M field in this paper is half of the one in Ref. [29].

We should note that, in the above expression, the mean fields σ_0 , ω , and ρ are solutions of the stationary conditions

$$0 = \frac{\partial \Omega}{\partial \sigma_0} = -\bar{\mu}^2 \sigma_0 + \lambda_4 \sigma_0^3 - \lambda_6 \sigma_0^5 - m_\pi^2 f_\pi + 2 \sum_{i,N} \frac{\partial m_N^{(i)}}{\partial \sigma_0} \int \frac{d^3 k}{(2\pi)^3} \frac{m_N^{(i)}}{E_N^{(i)}} \theta(\bar{\mu}_N^{(i)} - E_N^{(i)}), \quad (20)$$

$$0 = \frac{\partial \Omega}{\partial \omega} = -m_\omega^2 \omega + g_\omega \rho_B, \quad (21)$$

$$0 = \frac{\partial \Omega}{\partial \rho} = -m_\rho^2 \rho + g_\rho \rho_I, \quad (22)$$

where

$$\rho_B = \sum_i (\rho_p^{(i)} + \rho_n^{(i)}), \quad \rho_I = \sum_i \frac{\rho_p^{(i)} - \rho_n^{(i)}}{2}, \quad (23)$$

with

$$\rho_N^{(i)} = 2 \int \frac{d^3 k}{(2\pi)^3} \theta(\bar{\mu}_N^{(i)} - E_N^{(i)}). \quad (24)$$

B. Saturation properties at normal nuclear density

In this subsection, we provide formulas to calculate several physical quantities of nuclear matter at normal nuclear density.

From the thermodynamic potential obtained in the previous section, the baryon number density and the isospin density are calculated as

$$\rho_B = -\left(\frac{\partial \Omega}{\partial \mu_B}\right)_{\mu_I}, \quad \rho_I = -\left(\frac{\partial \Omega}{\partial \mu_I}\right)_{\mu_B}, \quad (25)$$

where $(\)_{\mu_I}$ implies that the derivative in terms of μ_B is taken with fixed μ_I , and similarly for $(\)_{\mu_B}$. One can easily confirm that ρ_B and ρ_I in Eq. (25) agree with those in Eq. (23). The saturation density ρ_0 is calculated as

$$\rho_0 = \rho_B(\mu_B = \mu_0, \mu_I = 0), \quad (26)$$

where μ_0 is the value of the baryon number chemical potential at the saturation point.

The pressure of the system is given by

$$P = -\Omega. \quad (27)$$

From the thermodynamic relation, the energy density is obtained as

$$\epsilon = -P + \mu_B \rho_B + \mu_I \rho_I. \quad (28)$$

Then, the binding energy is given by

$$\begin{aligned} E_{\text{bind}, \rho_0} &= -\left(\frac{E}{A}\right)_{\mu_B=\mu_0, \mu_I=0} - m_N \\ &= -\left(\frac{\epsilon}{\rho_B}\right)_{\mu_B=\mu_0, \mu_I=0} - m_N. \end{aligned} \quad (29)$$

From this, μ_0 in Eq. (26) is given as

$$\mu_0 = m_N^{(1)} - E_{\text{bind}, \rho_0}, \quad (30)$$

where $m_N^{(1)}$ is the mass of lightest nucleon. We note that, using the above conditions, we can easily show that the pressure at normal nuclear density vanishes:

$$P(\mu_B = \mu_0, \mu_I = 0) = 0. \quad (31)$$

The incompressibility is calculated as

$$K = 9\rho_B^2 \frac{\partial^2(\epsilon/\rho_B)}{\partial \rho_B^2} \Big|_{\rho_B=\rho_0} = 9\rho_B \frac{\partial \mu_B}{\partial \rho_B} \Big|_{\rho_B=\rho_0} \quad (32)$$

The symmetry energy per nucleon is given as

$$E_{\text{sym}} = \frac{1}{2} \frac{\partial^2(\epsilon/\rho_B)}{\partial \delta^2} \Big|_{\delta=0} = \frac{\rho_B}{8} \frac{\partial \mu_I}{\partial \rho_I} \Big|_{\rho_I=0}, \quad (33)$$

where δ is an asymmetric parameter defined as

$$\delta \equiv \frac{\rho_p - \rho_n}{\rho_B} = \frac{2\rho_I}{\rho_B}. \quad (34)$$

From Eq. (23), this is calculated as

$$E_{\text{sym}} = \frac{\rho_B}{8} \left(\frac{2\pi^2}{\sum_{N,i} k_{FN}^{(i)} E_{FN}^{(i)}} + \frac{g_\rho^2}{m_\rho^2} \right), \quad (35)$$

where the summation is taken over $N = p, n$ and $i = 1, 2, 3, 4$, and $k_{FN}^{(i)}$ and $E_{FN}^{(i)}$ are the Fermi momentum and Fermi energy of the nucleon. The slope parameter L is given by

$$L = 3\rho_B \frac{\partial E_{\text{sym}}(\rho_B)}{\partial \rho_B}. \quad (36)$$

Here, we assume that only the lightest nucleon exist in the nuclear matter at normal nuclear density. Then, this is reduced to

$$L = 3\rho_B \frac{\partial E_{\text{sym}}}{\partial \rho_B} \Big|_{\rho_B=\rho_0} \quad (37)$$

$$= 3\rho_0 \left[\frac{1}{8} \left(\frac{2\pi^2}{k_F E_F} + \frac{g_\rho^2}{m_\rho^2} \right) - \frac{\pi^2 (2k_F^2 + (m_N^*)^2)}{24k_F E_F^3} \right], \quad (38)$$

where $E_F = \bar{\mu}_B$ is the Fermi energy of the lightest nucleon, and k_F is the Fermi momentum, $k_F = \sqrt{\bar{\mu}_B^2 - (m_N^*)^2}$.

C. Neutron star matter and tidal deformability

In this subsection, we construct neutron star matter based on the model introduced in Sec. II. Here we assume that there are no hyperons and quarks in the matter constructed below.

To construct the neutron star matter, we introduce the electron and muon into matter, and require conditions for the charge neutrality and the beta equilibrium. The charge neutrality condition is written as

$$\sum_i \rho_p^{(i)} = \rho_e + \rho_\mu, \quad (39)$$

where $\rho_p^{(i)}$ is given in Eq. (24). The electron density and the muon density are given by

$$\rho_l = 2 \int \frac{d^3 k}{(2\pi)^3} \theta(\mu_l - E_l) \quad (l = e, \mu), \quad (40)$$

where μ_l is the corresponding chemical potential and

$$E_l = \sqrt{k^2 + m_l^2}, \quad (41)$$

with m_l being the lepton mass. Here we assume that the lepton masses in the neutron star matter are the same as those in vacuum. The chemical potentials for leptons satisfy the chemical equilibrium conditions

$$-\mu_l = \mu_e = \mu_\mu. \quad (42)$$

The mass and radius of neutron star are determined by solving the Tolman-Oppenheimer-Volkov (TOV) equations [46,47] given by

$$\begin{aligned} \frac{dP(r)}{dr} &= -\frac{\epsilon(r) + P(r)}{r[r - 2M(r)]} [M(r) + 4\pi^2 r^3 P(r)], \\ \frac{dM(r)}{dr} &= 4\pi^2 r^2 \epsilon(r). \end{aligned} \quad (43)$$

The solution of the above TOV equations determines the radius R and the mass M of the neutron star as

$$P(r=R) = 0, \quad M = M(r=R). \quad (44)$$

The dimensionless tidal deformability is defined as [48–50]

$$\Lambda = \frac{2}{3} k_2 C^{-5}, \quad (45)$$

where $C = M/R$ is the compactness parameter and k_2 is the tidal Love number calculated by

$$\begin{aligned} k_2 &= \frac{8C^5}{5} (1 - 2C)^2 [2 + 2C(y_R - 1) - y_R] \\ &\times [2C\{6 - 3y_R + 3C(5y_R - 8)\} \\ &+ 4C^3\{13 - 11y_R + C(3y_R - 2) + 2C^2(1 + y_R)\} \\ &+ 3(1 - 2C)^2\{2 - y_R + 2C(y_R - 1)\ln(1 - 2C)\}]^{-1}. \end{aligned} \quad (46)$$

In this expression, the quantity $y_R = y(r=R)$ is obtained by solving the following differential equation:

$$r \frac{dy(r)}{dr} + y(r)^2 + y(r)F(r) + r^2 + r^2 Q(r) = 0, \quad (47)$$

where

$$F(r) = \frac{r - 4\pi r^3 [\epsilon(r) - P(r)]}{r - 2M(r)},$$

TABLE I. Physical inputs used to determine the couplings of nucleons to scalar and pseudoscalar mesons. Units of masses and widths are in MeV. Note that we adopt the restriction of $-0.25 \leq g_A(1535) \leq 0.25$ from the lattice analysis [51] showing $g_A(1535) \sim \mathcal{O}(0.1)$.

	Mass	Width [$\Gamma_{N^* \rightarrow N\pi}$]	Axial charge
$N(939)$	939		1.272
$N(1440)$	1430	228	
$N(1535)$	1535	68	-0.25 – 0.25 [lat]
$N(1650)$	1655	84 [to $N(939)$ 22 [to $N(1440)$]	0.55 [lat]

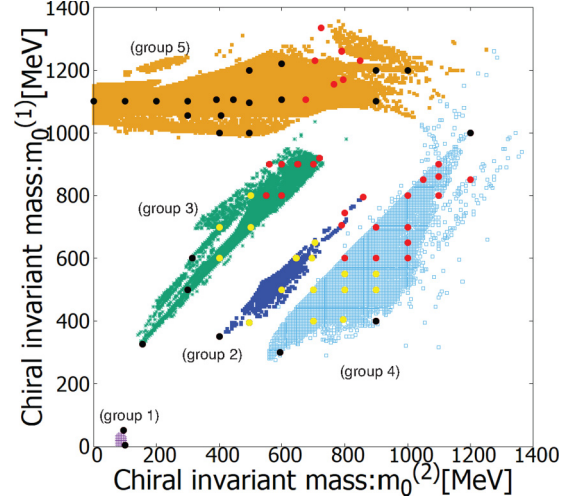


FIG. 1. Allowed region for two chiral invariant masses. Painted regions indicate the solutions which reproduce the physical inputs at vacuum shown in Table I as obtained in Ref. [17]. For combinations of two chiral invariant masses indicated by black, yellow, and red points, we checked whether the saturation properties are satisfied. For black points, the saturation properties of normal nuclear matter are not satisfied (see Sec. IV A). For combinations indicated by yellow and red points, we calculate the tidal deformability. For the yellow points the obtained tidal deformability does not satisfy the constraint obtained by GW170817, while the predictions for red points satisfy the constraints (see Sec. IV B).

$$\begin{aligned} Q(r) &= \frac{4\pi r (5\epsilon(r) + 9P(r) + \frac{\epsilon(r)+P(r)}{\partial P(r)/\partial \epsilon(r)} - \frac{6}{4\pi r^2})}{r - 2M(r)} \\ &- 4 \left[\frac{M(r) + 4\pi r^3 P(r)}{r^2 - 2M(r)r} \right]^2. \end{aligned} \quad (48)$$

The gravitational wave GW170817 was measured from a binary neutron star merger, so that it gives an constraint to the binary dimensionless tidal deformability, defined as

$$\tilde{\Lambda} = \frac{16}{13} \frac{(M_1 + 12M_2)M_1^4 \Lambda_1 + (M_2 + 12M_1)M_2^4 \Lambda_2}{(M_1 + M_2)^5}. \quad (49)$$

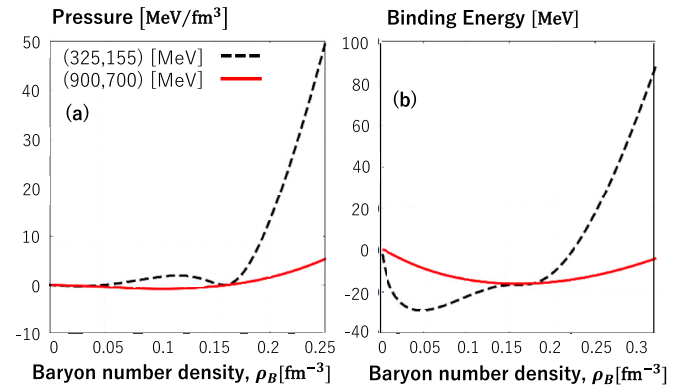


FIG. 2. Density dependencies of the pressure (left panel) and the binding energy (right panel). Black dashed curves are for $(m_0^{(1)}, m_0^{(2)}) = (325, 155)$ MeV, and the red solid curves are for $(900, 700)$ MeV.

TABLE II. Inputs values of the saturation density ρ_0 , the binding energy E_{bind,ρ_0} , the incompressibility K , and the symmetry energy E_{sym} at normal nuclear density. Unit of ρ_0 is fm^{-3} and units of others are MeV.

ρ_0	E_{bind,ρ_0}	K	E_{sym}
0.16	-16	240	31

where Λ_i ($i = 1, 2$) is the tidal deformability of each neutron star.

IV. NUMERICAL ANALYSIS

In Ref. [17], we determined ten couplings of nucleons to scalar and pseudoscalar mesons from ten physical inputs shown in Table I for fixed values of two chiral invariant masses and the pion decay constant $f_\pi = 92.4$ MeV. In the analysis, we varied the values of the chiral invariant masses $m_0^{(1)}$ and $m_0^{(2)}$ in 5 MeV steps from 0 to 1500 MeV and then fixed the other parameters from masses, partial decay widths, and axial charges. It was shown that only certain combinations of the two masses can reproduce these parameters as shown in Fig. 1. In this figure, we group the solutions into regions, indicated by the purple + symbols (group 1), blue ■ symbols (group 2), light green × symbols (group 3), light blue □ symbols (group 4), and yellow ■ symbols (group 5). In the following we shall show that some regions are excluded by requiring the saturation properties of normal nuclear matter and the tidal deformability constraint from the observation of GW170817 [37–39]. Here we assume that all the model parameters do not have any density dependence.

A. Saturation properties

In addition to the parameters determined in Ref. [17] at vacuum, as explained at the beginning of this section, we use the masses of ρ and ω mesons as

$$m_\omega = 783 \text{ MeV}, \quad m_\rho = 775 \text{ MeV}. \quad (50)$$

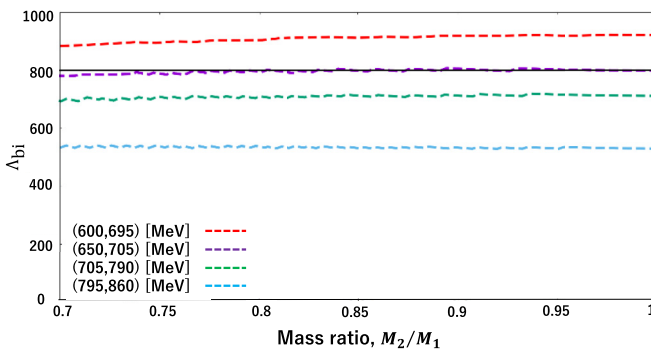


FIG. 3. Binary dimensionless tidal deformability ($\Lambda_{\text{bi}} \equiv \tilde{\Lambda}$) for several choices of two chiral invariant masses in group 2. The horizontal axis shows the ratio of two masses of neutron stars. Here we use the constraint of the mass ratio, $0.7 < M_2/M_1 < 1$ [37,54]. The dashed curves, from top to bottom, are for $(m_0^{(1)}, m_0^{(2)}) = (600, 695)$, $(650, 705)$, $(705, 790)$, $(795, 860)$ MeV, respectively. The black solid line at $\tilde{\Lambda} = 800$ is the upper bound of the constraint from the observation of GW170817 [37,54].

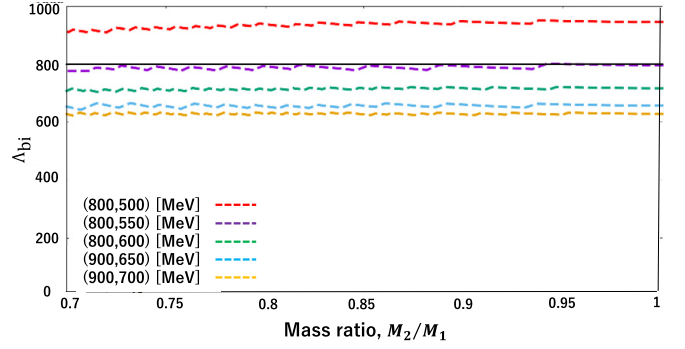


FIG. 4. Binary dimensionless tidal deformability ($\Lambda_{\text{bi}} \equiv \tilde{\Lambda}$) for several choices of two chiral invariant masses in group 3. The dashed curves, from top to bottom, are for $(m_0^{(1)}, m_0^{(2)}) = (800, 500)$, $(800, 550)$, $(800, 600)$, $(900, 650)$, $(900, 700)$ MeV, respectively.

Then, for fixed values of two chiral invariant masses, we determine four parameters, g_ω , g_ρ , λ_4 , and λ_6 to reproduce the saturation density, the binding energy, the incompressibility, and the symmetry energy at normal nuclear density shown in Table II.

We used the combinations of two chiral invariant masses as shown by black, yellow, and red points in Fig. 1, and found that the saturation properties cannot be reproduced for the combinations indicated by the black points. Let us explain the reason why we excluded the combinations where both the chiral invariant masses are small. For this purpose, we plot the density dependencies of the pressure and energy density for $(m_0^{(1)}, m_0^{(2)}) = (325, 155)$ MeV (black dashed curves), which we excluded, together with $(900, 700)$ MeV (red curves) which satisfies the saturation properties, in Fig. 2. Although both combinations satisfy $P = 0$ and $E/A - m_N = -16$ MeV at $\rho_0 = 0.16 \text{ fm}^{-3}$, the black dashed curves show that the binding energy is not minimized at ρ_0 and there is a global minimum around $\rho_B \approx 0.05 \text{ fm}^{-3}$. This implies that the matter at ρ_0 is not stable. This is because, for small chiral invariant masses, the coupling of the nucleon to σ is large, and the attractive force is strong.

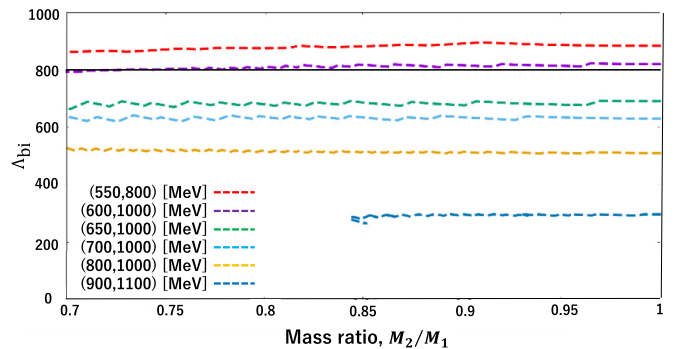


FIG. 5. Binary dimensionless tidal deformability ($\Lambda_{\text{bi}} \equiv \tilde{\Lambda}$) for several choices of two chiral invariant masses in group 4. The dashed curves, from top to bottom, are for $(m_0^{(1)}, m_0^{(2)}) = (550, 800)$, $(600, 1000)$, $(650, 1000)$, $(700, 1000)$, $(800, 1000)$, $(900, 1000)$ MeV, respectively.

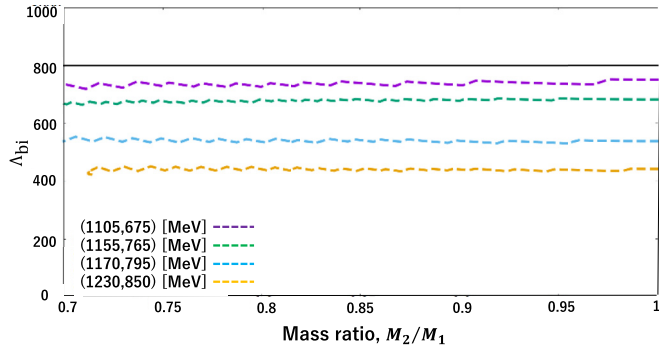


FIG. 6. Binary dimensionless tidal deformability ($\Lambda_{\text{bi}} \equiv \tilde{\lambda}$) for several choices of two chiral invariant masses in group 5. The dashed curves, from top to bottom, are for $(m_0^{(1)}, m_0^{(2)}) = (1105, 675)$, $(1155, 765)$, $(1170, 795)$, $(1230, 850)$ MeV, respectively.

A similar situation occurs when one of two chiral invariant masses is small. When both the chiral invariant masses are very large, on the other hand, the attractive force is too weak to keep the matter.

B. Tidal deformability

In this subsection, we construct the neutron star matter and calculate the tidal deformability using the formulas shown in the previous section. Here we assume that there are no hyperons and quarks in the matter.

When we solve the TOV equation (43), we use the equation of state (EOS) obtained from the present model for $\rho_B > 0.1 \text{ fm}^{-3}$, while we use the EOS given in Refs. [52,53] for $\rho_B < 0.1 \text{ fm}^{-3}$, regarding this region as the crust. Then, we calculate the binary tidal deformability for the Chirp mass of

$$M_{\text{Chirp}} = \frac{(M_1 M_2)^{3/5}}{(M_1 + M_2)^{1/5}} = 1.118 M_{\odot}, \quad (51)$$

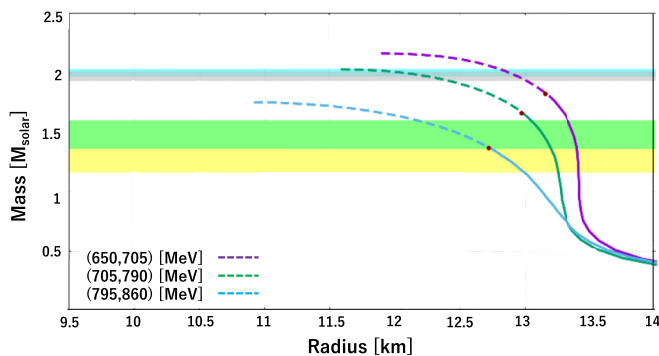


FIG. 7. Relation between the mass and radius of neutron stars for several combinations of two chiral invariant masses in group 2. The curves are for $(m_0^{(1)}, m_0^{(2)}) = (650, 705)$, $(705, 790)$, $(795, 860)$ MeV from top to bottom. Solid curves imply that the central density ρ_c is smaller than three times normal nuclear matter density, $\rho_c < 3\rho_0$, and the dashed curves are for $\rho_c > 3\rho_0$. Dots on the curves express that the central density is three times the normal nuclear density, $\rho_c = 3\rho_0$.

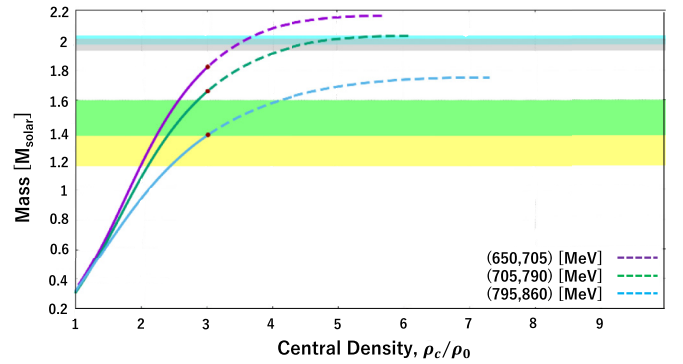


FIG. 8. Relation between the mass and central density of neutron stars for several combinations of two chiral invariant masses in group 2. The curves are for $(m_0^{(1)}, m_0^{(2)}) = (650, 705)$, $(705, 790)$, $(795, 860)$ MeV from top to bottom.

where M_{\odot} is the solar mass. We show the resultant values of the binary tidal deformability for several combinations of two chiral invariant masses for group 2 in Fig. 3. Here the dashed curves, from top to bottom, are for $(m_0^{(1)}, m_0^{(2)}) = (600, 695)$, $(650, 705)$, $(705, 790)$, and $(795, 860)$ MeV, respectively. We also plotted the black solid line at $\tilde{\lambda} = 800$, which we regard as the upper bound of the constraint from the observation of GW170817 [37,54]. Figure 3 shows that the $\tilde{\lambda}$ become smaller for larger chiral invariant mass. This is because the EOS becomes softer for larger chiral invariant mass.

As a result, the constraint $\tilde{\lambda} < 800$ excludes the region where chiral invariant masses are small. For example, the combination $(m_0^{(1)}, m_0^{(2)}) = (600, 695)$ MeV is excluded, as one can see easily in Fig. 3.

We next show the predicted $\tilde{\lambda}$ for groups 3, 4, 5 in Figs. 4, 5, 6, respectively. One can easily see that $\tilde{\lambda}$ is larger for smaller chiral invariant masses, and the combinations $(m_0^{(1)}, m_0^{(2)}) = (800, 500)$, $(550, 800)$ MeV are excluded. We summarize the results in Fig. 1, where red points show that $\tilde{\lambda} < 800$ is satisfied while yellow points show that the combination of the chiral invariant masses is excluded. From this, we conclude that the chiral invariant masses must be larger than

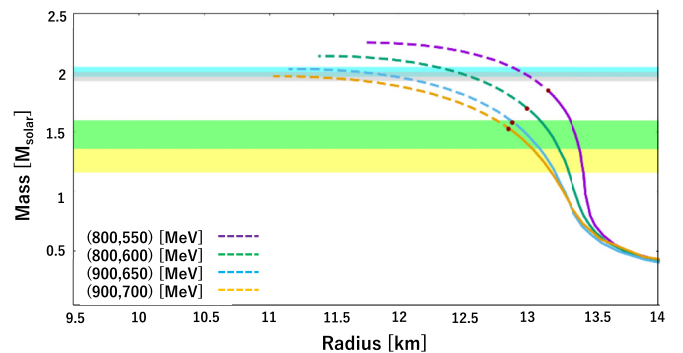


FIG. 9. Relation between the mass and radius of neutron stars for several combinations of two chiral invariant masses in group 3. The curves are for $(m_0^{(1)}, m_0^{(2)}) = (800, 550)$, $(800, 600)$, $(900, 600)$, $(900, 700)$ MeV from top to bottom.

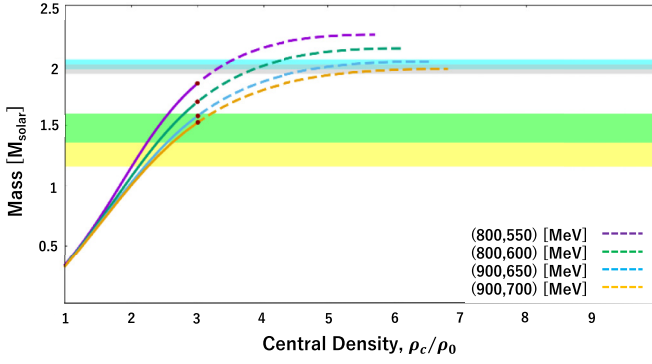


FIG. 10. Relation between the mass and central density of neutron stars for several combinations of two chiral invariant masses in group 3. The curves are for $(m_0^{(1)}, m_0^{(2)}) = (800, 550), (800, 600), (900, 600), (900, 700)$ MeV from top to bottom.

about 600 MeV to satisfy the tidal deformability constraint from the observation of GW170817.

C. M - R relation

In this subsection, we show our results for the M - R relation and the central density.

We plot the relation between neutron star mass and radius in Fig. 7 and the relation between the mass and the central density in Fig. 8 for several combinations of two chiral invariant masses $(m_0^{(1)}, m_0^{(2)})$ in group 2 which satisfy the constraint of the tidal deformability. Here, solid curves imply that the central density ρ_c is smaller than three times normal nuclear matter density, $\rho_c < 3\rho_0$, and the dashed curves are for $\rho_c > 3\rho_0$. Note that the combination $(m_0^{(1)}, m_0^{(2)}) = (795, 860)$ MeV is excluded, since the present prediction does not reproduce superheavy neutron stars with $2M_\odot$ mass [55,56]. However, we note that, in this study, we assume that the core of a neutron star is composed of protons, neutrons, and leptons only and that no hyperons, meson condensation, and quark degrees appear. We expect that the predictions shown by solid curves are not changed significantly, but those by dashed curves will be changed. Then, although the

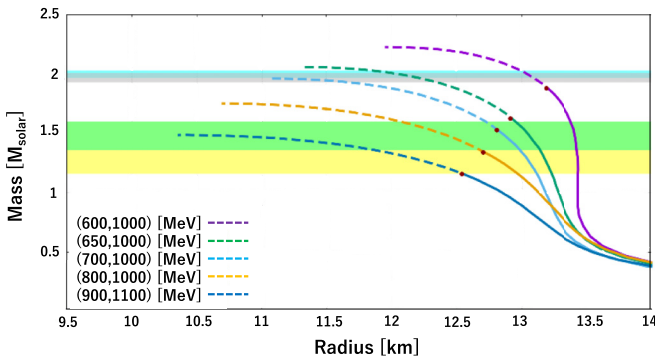


FIG. 11. Relation between the mass and radius of neutron stars for several combinations of two chiral invariant masses in group 4. The curves are for $(m_0^{(1)}, m_0^{(2)}) = (600, 1000), (650, 1000), (700, 1000), (800, 1000), (900, 1100)$ MeV from top to bottom.

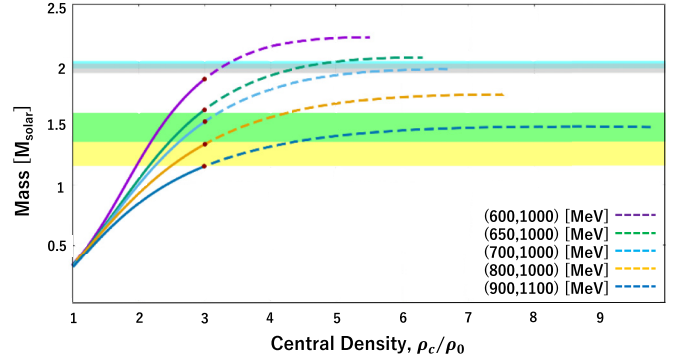


FIG. 12. Relation between the mass and central density of neutron stars for several combinations of two chiral invariant masses in group 4. The curves are for $(m_0^{(1)}, m_0^{(2)}) = (600, 1000), (650, 1000), (700, 1000), (800, 1000), (900, 1100)$ MeV from top to bottom.

present prediction for $(m_0^{(1)}, m_0^{(2)}) = (795, 860)$ MeV does not reproduce superheavy neutron stars with $2M_\odot$ mass [55,56], it will be changed by, e.g., including effects of quark degrees (see, e.g., Refs. [26,33,57–64]).

We also list the relations for groups 3–5 in Figs. 9–14. From these figures, we can see that the larger chiral invariant mass provides the softer EOS, leading to smaller radius and lighter mass. This is because the larger chiral invariant mass leads to smaller repulsive interaction.

D. Symmetry energy and slope parameter

In this subsection, we calculate the symmetry energy and the slope parameter in high density matter. The plots for $(m_0^{(1)}, m_0^{(2)}) = (900, 1100), (800, 1000), (600, 1000)$ MeV are shown in Fig. 15. We can see that three predictions are almost the same, and we checked that other predictions are similar. This is because, in Eq. (35), the second term in the parentheses is dominant and the symmetry energy is proportional to the baryon number density ρ_B . The slope parameters predicted here seem a little larger than the one constrained in Refs. [65,66]. In the present model, the large slope parameter causes the large radius of neutron stars.

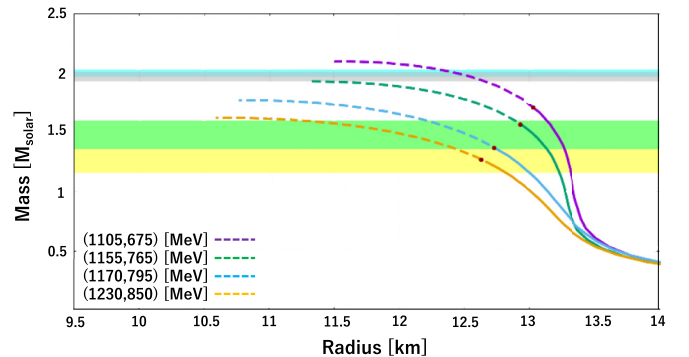


FIG. 13. Relation between the mass and radius of neutron stars for several combinations of two chiral invariant masses in group 5. The curves are for $(m_0^{(1)}, m_0^{(2)}) = (1105, 675), (1155, 765), (1170, 795), (1230, 850)$ MeV from top to bottom.

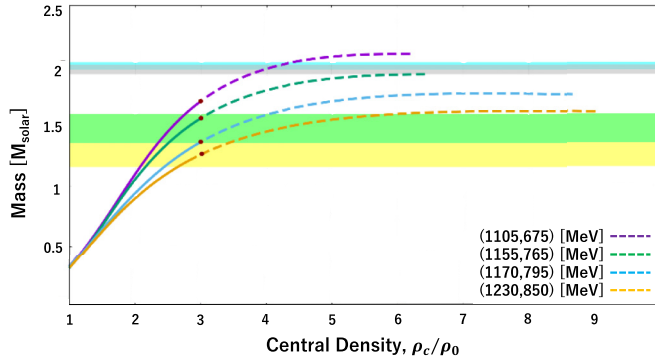


FIG. 14. Relation between the mass and central density of neutron stars for several combinations of two chiral invariant masses in group 5. The curves are for $(m_0^{(1)}, m_0^{(2)}) = (1105, 675), (1155, 765), (1170, 795), (1230, 850)$ MeV from top to bottom.

V. A SUMMARY AND DISCUSSION

In this paper, we constructed nuclear matter including neutron star matter from an extended parity doublet model, which we developed in the previous publication [17], wherein two sets of chiral representations having two chiral invariant masses are introduced. We showed that some combinations of two chiral invariant masses are excluded by requiring the saturation properties of normal nuclear matter: the saturation density, the binding energy, the incompressibility, and the symmetry energy. Then, we found that a further constraint on the chiral invariant masses is obtained from the tidal deformability determined by the observation of GW170817. Our result shows that the chiral invariant masses are larger than about 600 MeV, which is consistent with the constraint obtained in Ref. [36]. We also showed predictions of the mass-radius relation of neutron stars, as well as the symmetry energy and the slope parameter at high density.

In this paper, we regard the density region $\rho_B < 0.1 \text{ fm}^{-3}$ as the crust and use the EOS given in Refs. [52,53]. We studied the sensitivity of our results to the treatment of the crust by changing a way of connecting the EOS of the crust to the EOS of the core. We checked the following three different ways: (1) using crustal EOS for $\rho_B < 0.08 \text{ fm}^{-3}$; (2) using crustal EOS for $\rho_B < 0.13 \text{ fm}^{-3}$; (3) adopting a way proposed in Ref. [67] and regarding $0.08 < \rho_B < 0.16 \text{ fm}^{-3}$ as the crust-core connecting region. We found that the constraint on the chiral invariant masses is changed by 20–30 MeV at most.

In the present analysis, some of our predictions do not reproduce superheavy neutron stars with $2M_\odot$ [55,56], and a

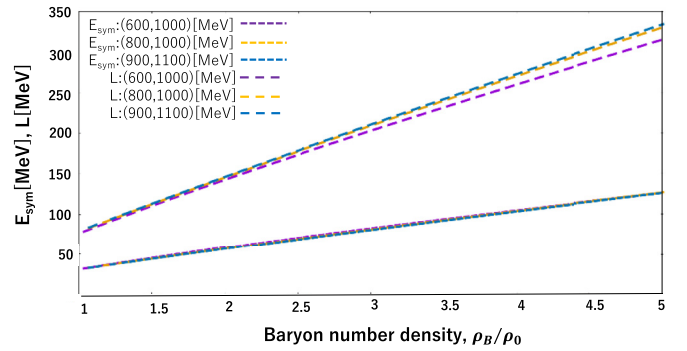


FIG. 15. Predicted symmetry energy (lower three curves) and slope parameter (upper three curves). The three curves for the symmetry energy are hard to be distinguished, while those for the slope parameter are for $(m_0^{(1)}, m_0^{(2)}) = (900, 1100), (800, 1000), (600, 1000)$ MeV, from top to bottom.

constraint from an x-ray burst given in Ref. [68]. However, we think that our model may not be applicable in the high-density region. It might be changed by, e.g., including effects of quark degrees (see, e.g., Refs. [26,33,57–64]). It will be interesting to obtain more constraints on the chiral invariant masses by including such effects.

The slope parameters predicted here seem a little larger than the one constrained in Ref. [65,66]. In the present model, the large slope parameter causes the large radius of neutron stars, which is comparable with the results in, e.g., Refs. [69–71], but larger than the ones in Refs. [61–63,72–74].

The large slope parameter implies that the proton fraction increases rapidly in the interior of the neutron star, which would lead to the rapid neutron star cooling via the direct Urca process (see, e.g., Ref. [75]). Observations of cooling neutron stars might provide more constraint to the invariant masses.

In our model, we include the six-point interaction of the σ meson. The existence of the six-point interaction might be driven by the violation of scale symmetry [76].

It will be interesting to apply the present analysis to study the modification of the spectrum of heavy-light mesons in dense matter, as was done in, e.g., Refs. [77,78].

ACKNOWLEDGMENTS

We would like to thank Youngman Kim, Young-Min Kim, Toru Kojo, Chang-Hwan Lee, Akira Ohnishi, and Chihiro Sasaki for valuable discussions and comments. The work of M.H. is supported in part by JSPS KAKENHI Grant No. 16K05345.

- [1] C. DeTar and T. Kunihiro, Linear σ model with parity doubling, *Phys. Rev. D* **39**, 2805 (1989).
- [2] D. Jido, Y. Nemoto, M. Oka, and A. Hosaka, Chiral symmetry for positive and negative parity nucleons, *Nucl. Phys. A* **671**, 471 (2000).
- [3] D. Jido, M. Oka, and A. Hosaka, Chiral symmetry of baryons, *Prog. Theor. Phys.* **106**, 873 (2001).

- [4] S. Gallas, F. Giacosa, and D. H. Rischke, Vacuum phenomenology of the chiral partner of the nucleon in a linear sigma model with vector mesons, *Phys. Rev. D* **82**, 014004 (2010).
- [5] Y. Nemoto, D. Jido, M. Oka, and A. Hosaka, Decays of $\frac{1}{2}^-$ baryons in chiral effective theory, *Phys. Rev. D* **57**, 4124 (1998).

- [6] H. X. Chen, V. Dmitrasinovic, A. Hosaka, K. Nagata, and S. L. Zhu, Chiral properties of baryon fields with flavor SU(3) symmetry, *Phys. Rev. D* **78**, 054021 (2008).
- [7] V. Dmitrasinovic, A. Hosaka, and K. Nagata, Nucleon axial couplings and $[(1/2, 0) \oplus (0, 1/2)] - [(1, 1/2) \oplus (1/2, 1)]$ chiral multiplet mixing, *Mod. Phys. Lett. A* **25**, 233 (2010).
- [8] V. Dmitrasinovic, A. Hosaka, and K. Nagata, A Lagrangian for the chiral $(1/2, 0) + (0, 1/2)$ quartet nucleon resonances, *Int. J. Mod. Phys. E* **19**, 91 (2010).
- [9] H. X. Chen, V. Dmitrasinovic, and A. Hosaka, Baryon fields with $U_L(3) \times U_R(3)$ chiral symmetry II: Axial currents of nucleons and hyperons, *Phys. Rev. D* **81**, 054002 (2010).
- [10] H. X. Chen, V. Dmitrasinovic, and A. Hosaka, Baryon fields with $U_L(3) \times U_R(3)$ chiral Symmetry III: Interactions with chiral $(3, \bar{3}) + (\bar{3}, 3)$ spinless mesons, *Phys. Rev. D* **83**, 014015 (2011).
- [11] J. Steinheimer, S. Schramm, and H. Stocker, Hadronic SU(3) parity doublet model for dense matter and its extension to quarks and the strange equation of state, *Phys. Rev. C* **84**, 045208 (2011).
- [12] H. X. Chen, V. Dmitrasinovic, and A. Hosaka, Baryons with $U_L(3) \times U_R(3)$ chiral symmetry IV: Interactions with chiral $(8, 1) \oplus (1, 8)$ vector and axial-vector mesons and anomalous magnetic moments, *Phys. Rev. C* **85**, 055205 (2012).
- [13] H. Nishihara and M. Harada, Extended Goldberger-Treiman relation in a three-flavor parity doublet model, *Phys. Rev. D* **92**, 054022 (2015).
- [14] L. Olbrich, M. Zétényi, F. Giacosa, and D. H. Rischke, Three-flavor chiral effective model with four baryonic multiplets within the mirror assignment, *Phys. Rev. D* **93**, 034021 (2016).
- [15] V. Dmitrašinović, H. X. Chen, and A. Hosaka, Baryon fields with $U_L(3) \times U_R(3)$ chiral symmetry. V. Pion-nucleon and kaon-nucleon Σ terms, *Phys. Rev. C* **93**, 065208 (2016).
- [16] C. Sasaki, Parity doubling of baryons in a chiral approach with three flavors, *Nucl. Phys. A* **970**, 388 (2018).
- [17] T. Yamazaki and M. Harada, Chiral partner structure of light nucleons in an extended parity doublet model, *Phys. Rev. D* **99**, 034012 (2019).
- [18] T. Hatsuda and M. Prakash, Parity doubling of the nucleon and first order chiral transition in dense matter, *Phys. Lett. B* **224**, 11 (1989).
- [19] D. Zschesche, L. Tolos, J. Schaffner-Bielich, and R. D. Pisarski, Cold, dense nuclear matter in a SU(2) parity doublet model, *Phys. Rev. C* **75**, 055202 (2007).
- [20] V. Dexheimer, S. Schramm, and D. Zschesche, Nuclear matter and neutron stars in a parity doublet model, *Phys. Rev. C* **77**, 025803 (2008).
- [21] V. Dexheimer, G. Pagliara, L. Tolos, J. Schaffner-Bielich, and S. Schramm, Neutron stars within the SU(2) parity doublet model, *Eur. Phys. J. A* **38**, 105 (2008).
- [22] C. Sasaki and I. Mishustin, Thermodynamics of dense hadronic matter in a parity doublet model, *Phys. Rev. C* **82**, 035204 (2010).
- [23] C. Sasaki, H. K. Lee, W. G. Paeng, and M. Rho, Conformal anomaly and the vector coupling in dense matter, *Phys. Rev. D* **84**, 034011 (2011).
- [24] S. Gallas, F. Giacosa, and G. Pagliara, Nuclear matter within a dilatation-invariant parity doublet model: the role of the tetraquark at nonzero density, *Nucl. Phys. A* **872**, 13 (2011).
- [25] W. G. Paeng, H. K. Lee, M. Rho, and C. Sasaki, Dilaton-limit fixed point in hidden local symmetric parity doublet model, *Phys. Rev. D* **85**, 054022 (2012).
- [26] V. Dexheimer, J. Steinheimer, R. Negreiros, and S. Schramm, Hybrid stars in an SU(3) parity doublet model, *Phys. Rev. C* **87**, 015804 (2013).
- [27] W. G. Paeng, H. K. Lee, M. Rho, and C. Sasaki, Interplay between ω -nucleon interaction and nucleon mass in dense baryonic matter, *Phys. Rev. D* **88**, 105019 (2013).
- [28] S. Benic, I. Mishustin, and C. Sasaki, Effective model for the QCD phase transitions at finite baryon density, *Phys. Rev. D* **91**, 125034 (2015).
- [29] Y. Motohiro, Y. Kim, and M. Harada, Asymmetric nuclear matter in a parity doublet model with hidden local symmetry, *Phys. Rev. C* **92**, 025201 (2015); **95**, 059903(E) (2017).
- [30] A. Mukherjee, J. Steinheimer, and S. Schramm, Higher-order baryon number susceptibilities: Interplay between the chiral and the nuclear liquid-gas transitions, *Phys. Rev. C* **96**, 025205 (2017).
- [31] D. Suenaga, Examination of $N^*(1535)$ as a probe to observe the partial restoration of chiral symmetry in nuclear matter, *Phys. Rev. C* **97**, 045203 (2018).
- [32] Y. Takeda, Y. Kim, and M. Harada, Catalysis of partial chiral symmetry restoration by Δ matter, *Phys. Rev. C* **97**, 065202 (2018).
- [33] A. Mukherjee, S. Schramm, J. Steinheimer, and V. Dexheimer, The application of the quark-hadron chiral parity-doublet model to neutron star matter, *Astron. Astrophys.* **608**, A110 (2017).
- [34] M. Marczenko and C. Sasaki, Net-baryon number fluctuations in the hybrid quark-meson-nucleon model at finite density, *Phys. Rev. D* **97**, 036011 (2018).
- [35] H. Abuki, Y. Takeda, and M. Harada, Dual chiral density waves in nuclear matter, *EPJ Web Conf.* **192**, 00020 (2018).
- [36] M. L. Marczenko, D. Blaschke, K. Redlich, and C. Sasaki, Chiral symmetry restoration by parity doubling and the structure of neutron stars, *Phys. Rev. D* **98**, 103021 (2018).
- [37] B. P. Abbott *et al.* (LIGO Scientific and Virgo Collaborations), GW170817: Observation of Gravitational Waves from a Binary Neutron Star Inspiral, *Phys. Rev. Lett.* **119**, 161101 (2017).
- [38] B. P. Abbott *et al.*, Multi-messenger observations of a binary neutron star merger, *Astrophys. J.* **848**, L12 (2017).
- [39] B. P. Abbott *et al.* (LIGO Scientific and Virgo Collaborations), GW170817: Measurements of Neutron Star Radii and Equation of State, *Phys. Rev. Lett.* **121**, 161101 (2018).
- [40] I. J. Shin, W. G. Paeng, M. Harada, and Y. Kim, Nuclear structure in parity doublet model, [arXiv:1805.03402](https://arxiv.org/abs/1805.03402).
- [41] G. Aarts, C. Allton, D. De Boni, S. Hands, B. Jäger, C. Praki, and J. I. Skullerud, Light baryons below and above the deconfinement transition: Medium effects and parity doubling, *J. High Energy Phys.* **06** (2017) 034.
- [42] G. Aarts, C. Allton, D. de Boni, S. Hands, B. Jäger, C. Praki, and J. I. Skullerud, Baryons in the plasma: In-medium effects and parity doubling, *EPJ Web Conf.* **171**, 14005 (2018).
- [43] G. Aarts, C. Allton, D. De Boni, and B. Jäger, Hyperons in thermal QCD: A lattice view, *Phys. Rev. D* **99**, 074503 (2019).
- [44] M. Bando, T. Kugo, and K. Yamawaki, Nonlinear realization and hidden local symmetries, *Phys. Rep.* **164**, 217 (1988).
- [45] M. Harada and K. Yamawaki, Hidden local symmetry at loop: A new perspective of composite gauge boson and chiral phase transition, *Phys. Rep.* **381**, 1 (2003).

- [46] R. C. Tolman, Static solutions of Einstein's field equations for spheres of fluid, *Phys. Rev.* **55**, 364 (1939).
- [47] J. R. Oppenheimer and G. M. Volkoff, On massive neutron cores, *Phys. Rev.* **55**, 374 (1939).
- [48] T. Hinderer, Tidal Love numbers of neutron stars, *Astrophys. J.* **677**, 1216 (2008).
- [49] T. Hinderer, B. D. Lackey, R. N. Lang, and J. S. Read, Tidal deformability of neutron stars with realistic equations of state and their gravitational wave signatures in binary inspiral, *Phys. Rev. D* **81**, 123016 (2010).
- [50] T. Malik, N. Alam, M. Fortin, C. Providência, B. K. Agrawal, T. K. Jha, B. Kumar, and S. K. Patra, GW170817: Constraining the nuclear matter equation of state from the neutron star tidal deformability, *Phys. Rev. C* **98**, 035804 (2018).
- [51] T. T. Takahashi and T. Kunihiro, Axial charges of $N(1535)$ and $N(1650)$ in lattice QCD with two flavors of dynamical quarks, *Phys. Rev. D* **78**, 011503 (2008).
- [52] G. Baym, C. Pethick, and P. Sutherland, The ground state of matter at high densities: Equation of state and stellar models, *Astrophys. J.* **170**, 299 (1971).
- [53] B. K. Sharma, M. Centelles, X. Viñas, M. Baldo, and G. F. Burgio, Unified equation of state for neutron stars on a microscopic basis, *Astron. Astrophys.* **584**, A103 (2015).
- [54] B. P. Abbott *et al.* (LIGO Scientific and Virgo Collaborations), Properties of the Binary Neutron Star Merger GW170817, *Phys. Rev. X* **9**, 011001 (2019).
- [55] P. Demorest, T. Pennucci, S. Ransom, M. Roberts, and J. Hessels, A two-solar-mass neutron star measured using Shapiro delay, *Nature (London)* **467**, 1081 (2010).
- [56] J. Antoniadis *et al.*, A massive pulsar in a compact relativistic binary, *Science* **340**, 6131 (2013).
- [57] K. Masuda, T. Hatsuda, and T. Takatsuka, Hadron-quark crossover and massive hybrid stars with strangeness, *Astrophys. J.* **764**, 12 (2013).
- [58] K. Masuda, T. Hatsuda, and T. Takatsuka, Hadron-quark crossover and massive hybrid stars, *Prog. Theor. Exp. Phys.* **2013**, 073D01 (2013).
- [59] K. Masuda, T. Hatsuda, and T. Takatsuka, Hadron-quark crossover and hot neutron stars at birth, *Prog. Theor. Exp. Phys.* **2016**, 021D01 (2016).
- [60] K. Masuda, T. Hatsuda, and T. Takatsuka, Hyperon puzzle, hadron-quark crossover and massive neutron stars, *Eur. Phys. J. A* **52**, 65 (2016).
- [61] T. Kojo, P. D. Powell, Y. Song, and G. Baym, Phenomenological QCD equation of state for massive neutron stars, *Phys. Rev. D* **91**, 045003 (2015).
- [62] T. Kojo, P. D. Powell, Y. Song, and G. Baym, Phenomenological QCD equations of state for neutron stars, *Nucl. Phys. A* **956**, 821 (2016).
- [63] G. Baym, T. Hatsuda, T. Kojo, P. D. Powell, Y. Song, and T. Takatsuka, From hadrons to quarks in neutron stars: A review, *Rep. Prog. Phys.* **81**, 056902 (2018).
- [64] X. Wu, A. Ohnishi, and H. Shen, Effects of quark-matter symmetry energy on hadron-quark coexistence in neutron-star matter, *Phys. Rev. C* **98**, 065801 (2018).
- [65] I. Tews, J. M. Lattimer, A. Ohnishi, and E. E. Kolomeitsev, Symmetry parameter constraints from a lower bound on neutron-matter energy, *Astrophys. J.* **848**, 105 (2017).
- [66] A. Ohnishi (private communication).
- [67] C. Y. Tsang, M. B. Tsang, P. Danielewicz, W. G. Lynch, and F. J. Fattoyev, Constraining neutron-star equation of state using heavy-ion collisions, [arXiv:1807.06571](https://arxiv.org/abs/1807.06571).
- [68] J. Nättilä, M. C. Miller, A. W. Steiner, J. J. E. Kajava, V. F. Suleimanov, and J. Poutanen, Neutron star mass and radius measurements from atmospheric model fits to X-ray burst cooling tail spectra, *Astron. Astrophys.* **608**, A31 (2017).
- [69] E. R. Most, L. R. Weih, L. Rezzolla, and J. Schaffner-Bielich, New Constraints on Radii and Tidal Deformabilities of Neutron Stars from GW170817, *Phys. Rev. Lett.* **120**, 261103 (2018).
- [70] F. J. Fattoyev, J. Piekarewicz, and C. J. Horowitz, Neutron Skins and Neutron Stars in the Multimessenger Era, *Phys. Rev. Lett.* **120**, 172702 (2018).
- [71] Y. M. Kim, Y. Lim, K. Kwak, C. H. Hyun, and C. H. Lee, Tidal deformability of neutron stars with realistic nuclear energy density functionals, *Phys. Rev. C* **98**, 065805 (2018).
- [72] A. W. Steiner, J. M. Lattimer, and E. F. Brown, The equation of state from observed masses and radii of neutron stars, *Astrophys. J.* **722**, 33 (2010).
- [73] J. M. Lattimer and A. W. Steiner, Constraints on the symmetry energy using the mass-radius relation of neutron stars, *Eur. Phys. J. A* **50**, 40 (2014).
- [74] H. Togashi, K. Nakazato, Y. Takehara, S. Yamamuro, H. Suzuki, and M. Takano, *Nucl. Phys. A* **961**, 78 (2017).
- [75] J. M. Lattimer, C. J. Pethick, M. Prakash, and P. Haensel, Direct URCA Process in Neutron Stars, *Phys. Rev. Lett.* **66**, 2701 (1991).
- [76] Y. L. Ma and M. Rho, Scale-chiral symmetry, ω meson and dense baryonic matter, *Phys. Rev. D* **97**, 094017 (2018).
- [77] M. Harada, Y. L. Ma, D. Suenaga, and Y. Takeda, Relation between the mass modification of the heavy-light mesons and the chiral symmetry structure in dense matter, *Prog. Theor. Exp. Phys.* **2017**, 113D01 (2017).
- [78] D. Suenaga, Spectral function for $\bar{D}_0^*(0^+)$ meson in isospin asymmetric nuclear matter with chiral partner structure, [arXiv:1805.01709](https://arxiv.org/abs/1805.01709).